Predicting the Structural Response of Free-Standing Spent Fuel Storage Casks Under Seismic Events

K.P. Singh, Ph.D., PE[1], Alan I. Soler, Ph.D.[1] and Mark Smith[2]

1) Holtec International, Marlton, NJ
2) Pacific Gas and Electric Company, Eureka, CA

ABSTRACT

A spent fuel storage cask installed on reinforced concrete pads in the free-standing configuration must be qualified for kinematic stability and stress compliance under the postulated Design Basis Earthquake for the facility. A dynamic analysis method to predict the response of a loaded cask subjected to 3-D seismic excitation is presented in this paper. The methodology permits parametric evaluation of variables such as cask-to-pad interface friction coefficient, fuel-to-storage cell gaps, fuel basket stiffness, and fuel compliance characteristics. A set of acceptance criteria to ensure stability with a margin of safety appropriate for a nuclear installation are also proposed for possible adoption by the regulatory authorities.

INTRODUCTION

In most cases, cask systems for storing spent nuclear fuel have been installed as free-standing structures on reinforced concrete pads. Installing the casks as free-standing structures on a concrete pad has the financial benefit in the form of a reduced implementation and future decommissioning costs, as well as the perceptional advantage of a "rootless" fuel storage facility. The physical disconnect between the cask and the pad has enabled the USNRC to enunciate a clear regulatory position with respect to storage casks which permits the holder of a Part 50 license to deploy an NRC-certified storage cask on its storage pad without further licensing reviews. Court interpretation of federal laws and regulations with respect to Part 72 provisions essentially permit the nuclear plant owner to establish a dry storage facility using an NRC-certified cask without exposure to potential delays from local intervention. Unencumbered of regulatory and intervenor intrusion, the so-called "Subpart K" ISFSI (acronym for Independent Spent Fuel Storage Installation) has been the vehicle of choice for nuclear plants seeking to employ dry storage. The USNRC has sought to control the quality of the site civil and architectural work (such as pouring of concrete) through on-site inspection and Information Notices [1]. The regulatory guidelines and implementation thus far appeared to have worked well.

From the structural standpoint, fuel storage casks of modern vintage designs consist of two discrete structures referred to as the "multi-purpose canister" (or MPC) and the "overpack". The overpack is typically a thick cylindrical structure with a circular footprint and a bolted top lid. The overpack houses the MPC in an upright configuration. The MPC is also of right circular cylinder silhouette. Inside the MPC, a "fuel basket" containing an array of square cross-section cavities holds the spent fuel assemblies. Figure 1 shows a pictorial view of the HI-STAR 100 overpack (recently certified by the USNRC) with its MPC partially inserted. A typical HI-STAR 100 MPC and its fuel basket are illustrated in Figures 2 and 3, respectively.

It is clear from the above description that from a structural standpoint, a cask system is a highly nonlinear system. In fact the cask is an assemblage of a number of structures; chief among them are the overpack, the MPC cylinder, the fuel basket, and an array of fuel assemblies, each one of which is a discrete structural component. These individual structures are arrayed in a cask system with small lateral gaps which would promote internal rattling during a vibratory terrestrial event. A rigorous prognostication of the response of such a complex structure under seismic inputs evidently requires a comparably sophisticated analysis model. However, even though the casks are installed as free-standing structures in relative close proximity to each other (four to eight feet apart), their kinematic stability under earthquakes has not been a matter of in-depth assessment and inquiry on the part of the cask designers or the USNRC. This is partly due to the fact that casks are relatively stubby structures which makes them reasonably stable under moderate tremors. The so-called Independent Spent Fuel Storage Installations (ISFSIs) to date have been located primarily in the regions of the country which have low "design basis earthquakes" (DBE). However, this condition is about to change as the plants in the western United States are forced to develop ISFSIs to meet their fuel storage needs or to undertake reactor decommissioning efforts. High earthquake sites must explore the consequences of DBEs at their ISFSIs as an important part of their *safety evaluation*. For reasons that we explain later, a static force balance method, used to qualify casks under earthquakes, would fail to satisfy the needs for the high seismic sites. A comprehensive analysis of the interaction of the cask structure with its concrete base during the seismic event is an essential prerequisite for establishing the seismic safety for such sites. Earthquakes are, in essence, vibratory events which can be represented by three orthogonal accelerograms. To properly characterize the seismic characteristics of the cask, it is necessary to perform a dynamic simulation under three simultaneous orthogonal vibratory excitations. One of the objectives of this paper is to present a dynamic analysis methodology suitable for analyzing loaded spent fuel storage casks on reinforced concrete ISFSIs. Another objective is to propose a procedure that may be used to determine seismic stability of casks in an efficient manner.

Before proceeding with the formulation and solution of the seismic problem, it is helpful to survey the current design practice.

STATIC EQUILIBRIUM PROCEDURE

The design practice for analyzing stability of casks until now has relied on static moment equilibrium. The seismic excitation is treated as a constant static load. The condition of "incipient tipping" of the cask is examined by postulating that a net horizontal load acting at the cask centroid can be balanced only by the vertical reaction acting at the outermost point of the contact interface. Therefore, if H^* is the height of the centroid of the HI-STAR 100 System above the contact patch, then the overturning static moment is

$$W\ H^*\ a_H$$

where W is the cask weight and a_H is the seismic amplifier so that Wa_H is the horizontal inertia load due to seismic effects. The overturning moment is balanced by a vertical reaction force, acting at the outermost contact patch radial location r. For a conservative result, it is assumed that the maximum overturning moment occurs at the instant when the vertical seismic load is directed upward, and that the vertical seismic load is equal to the horizontal seismic load. Therefore, the moment that resists "incipient tipping" is

$$W(1-a_H)\ r$$

where we have tacitly assumed the acceleration level to be equal in the horizontal and vertical directions. Equating the two expressions to satisfy moment equilibrium yields

$$WH^*a_H \le W(1-a_H)\ r$$

or, after canceling W, and solving for a_H

$$a_H \le \frac{r}{H^* + r}$$

To illustrate the application of the above formula and of the dynamic analysis methodology proposed herein, we consider the case of the HI-STAR 100 dual-purpose cask system (Figure 1) certified by the USNRC under Docket Numbers 72-1008 for storage and 71-9261 for transport. The data for the contact patch radius r and height of the C.G. are obtained from the Topical Safety Analysis Report for HI-STAR 100 [2].

We have r = 41.625", and H^* = 101.1"

which yields

$$g \le 0.292$$

Stated in words, static equilibrium indicates that a coincident vertical and horizontal seismic acceleration equal to 0.292 times the acceleration due to gravity will not tip the HI-STAR 100 System.

The limitations of this procedure are quite apparent. An earthquake is a vibratory event, not a static time-invariant load. The moment equilibrium pre-supposes that the cask will not slide, a strenuous assumption for an ISFSI open to the elements including rain, snow, and other interface "lubricants" which may induce sliding instead of overturning. To eliminate the limitations (and uncertainties) inherent to the static analysis, it is necessary to solve the dynamic problem appropriate to earthquake motions using a suitable mathematical model, which we describe in the next section.

SOLUTION PROCEDURE

A free-standing cask is an epitome of a nonlinear structure. The contents of the cask, namely the stored spent nuclear fuel, the fuel basket, and the multi-purpose canister (MPC), are installed with clearances, which permits them to "rattle" inside the cask during a seismic event. To predict the response of this class of structures, the most widely used analysis methodology is the so-called "time-history" method [6].

The time-history method essentially consists of discretizing the structure into a finite number of degrees of freedom (DOF), establishing the structural connectivities among the DOFs and writing the second order matrix differential equations of motion to quantify the system's response to the prescribed seismic stimuli. The time-history method has become a most widely used tool to analyze nonlinear structures in nuclear plants, such as spent fuel storage racks used in underwater storage of burned reactor fuel. The methodology for free-standing cask analysis presented in this paper, in fact, is a direct extension of a similar, previously published work on spent fuel racks [10].

An axiomatic fact in the nonlinear dynamic analysis is that the response of the structure from individual loadings cannot be summed linearly or by the traditional square-root-of-the-sum-of-square method common in linear simulations. The three orthogonal ground accelerations must be applied *simultaneously* to obtain a meaningful solution for the seismic response. Accordingly, in the dynamic analysis methodology presented herein, seismic accelerations in the three orthogonal directions are applied simultaneously to the slab supporting the cask system.

The methodology presented in this paper can be used to evaluate the response of a cask to a specified set of acceleration time-histories. However, to facilitate design work, it may be feasible to pre-qualify the cask for a "bounding earthquake". It is possible to accomplish this objective by using the concept of the response spectrum [3,4], as we explain below.

Design Basis Seismic excitation for a site is a complex function of a wide array of geophysical variables. Each specific ISFSI site has its own signature earthquake developed by the geotechnical engineers. The strength of an earthquake, however, is definitively portrayed by its response spectrum [3,4]. It is commonly recognized that the response of a structure to two seismic inputs can be reliably compared by examining their response spectra. If one spectrum uniformly envelopes another, then the response of the structure to the "enveloping" earthquake will bound that to the "enveloped" one. With this axiom in mind, the response spectrum defined by the USNRC, the so-called Reg. Guide 1.60 spectrum [3], was selected as the reference spectrum. A twenty-second synthetic time-history which envelopes the reference spectrum and the related power spectrum density function was developed in compliance with the provisions of NUREG-0800 [8]. Figures 4 to 6 show three artificial acceleration time-histories with ZPA = 1.00, all of which meet Reference [8] enveloping requirements. Furthermore, these time-histories are statistically independent of each other (defined as the cross correlation coefficient $\alpha_{ij} \leq 0.1$; i,j = 1,2,3). As shown in Figures 7 to 9, the response spectra corresponding to the synthetic time-histories bound the design spectra uniformly within the prescriptions of [8]. It is recognized that an infinite number of time-histories can be generated that will also satisfy the regulatory requirements [8]. It is assumed hereafter that an appropriate set of time-histories has been generated.

The next step in the analysis process is to develop a suitable dynamic model for the cask system. The cask dynamic model seeks to articulate a relatively rigid overpack containing an autonomous structure, namely, a multi-purpose canister (MPC) supported on an elastic foundation (ISFSI) with a defined interfacial coefficient-of-friction, μ. The structure to be analyzed is represented with sufficient degrees of freedom to capture its dynamic response accurately in the mathematical model. Figure 10 shows the dissasembled view of the HI-STAR 100 System modeled as a twenty-three degree of freedom system. Six degrees of freedom (6 DOF) describe the translation and rotation of the cask overpack as a rigid body; three translational (DOF 1-3) and three rotational (DOF 4-6) degrees of freedom are defined at the cask center of gravity location. The multi-purpose canister (MPC) is fully confined in the overpack; however, the small lateral and vertical gaps permit independent MPC canister (the shell, lid, and baseplate) motion relative to the overpack. Contained within the MPC shell and top and bottom closures is a multi-cell fuel basket which is a free-standing structure capable of vertical movement within the canister. Five degrees of freedom describe translation (DOF 7-9) and rotation (DOF 10-11) about two orthogonal horizontal axes of the MPC. Degrees of freedom 7,8,10, and 11 include the mass and inertia of both the MPC canister and the fuel basket. Degree of freedom 9 includes only the mass of the MPC canister as a separate degree of freedom used to describe the vertical motion of the fuel basket. The fuel assemblies contained within the MPC are typically very flexible components compared to the various structural components of the cask system; ten degrees of freedom describe the translation in the horizontal plane of each of five fuel assembly lumped masses located along the centerline of the system. As stated previously, the lumped masses represent *all* fuel assemblies stored in the cask system; the independent masses are located at the MPC top (DOF 12-13), the MPC three-quarter height (DOF 14-15), the MPC half-height (DOF 16-17), the MPC quarter-height (DOF 18-19), and the MPC bottom (DOF 20-21). The vertical motion of the totality of fuel assemblies is described by a single degree of freedom (DOF 22). Finally, the vertical movement of the fuel basket, within the MPC canister, is described by one translational degree of freedom (DOF 23). The structural resistance to the seismic loading is provided by a series of vertical compression-only gap elements, located around the periphery of the overpack

baseplate, which provide restoring moments when the cask system tends to overturn due to seismic forces. Associated with these vertical compression-only elements are piecewise linear friction elements which simulate the potential for sliding at the cask/pad interface locations if the lateral force at the time instant in question exceeds the normal force at that location. Figure 11 shows a typical interface location and the associated compression-only element with two horizontal friction elements. Also included in the model are compression-only elements to simulate the opening and closing of the small gaps between various cask components and between the fuel and the fuel basket. Representative gaps between the components are used in the simulation, and the contact stiffness between components are set at conservatively high values to maximize the impact loads.

The governing equations of motion are derived using the classical Lagrangian method [5,6] wherein the kinetic energy of the system is written in terms of the generalized coordinates of the problem. Performing certain partial differentiation operations on the kinetic energy, and equating the results of the operations to the appropriate generalized forces associated with each degree of freedom, yields the appropriate system equations of motion. In general terms, if K is defined as the system kinetic energy, then the equations of motion for the cask system can be written by differentiating the system kinetic energy and calculation and subsequent inspection of the extensions of the spring elements in the problem expressed in terms of generalized coordinates, as described below.

Referring to the nomenclature, the constituent components of the system kinetic energy can be written as follows:

a. Overpack

$$K_1 = \frac{1}{2} M_1 (\dot{q}_1^2 + \dot{q}_2^2 + \dot{q}_3^2) + \frac{1}{2} I_1 (\dot{q}_4^2 + \dot{q}_5^2) + \frac{1}{2} I_3 \dot{q}_6^2$$

b. MPC plus the Fuel Basket (except for the kinetic energy of fuel basket due to vertical motion)

$$K_2 = \frac{1}{2} M_2 (\dot{q}_7^2 + \dot{q}_8^2) + \frac{1}{2} M_3 \dot{q}_9^2 + \frac{1}{2} I_4 (\dot{q}_{10}^2 + \dot{q}_{11}^2)$$

c. MPC Fuel Basket - Vertical Motion

$$K_3 = \frac{1}{2} M_4 \dot{q}_{23}^2$$

d. Fuel Assembly Mass

$$K_4 = \frac{1}{2} M_f (\dot{q}_{12}^2 + \dot{q}_{13}^2 + \dot{q}_{14}^2 + \dot{q}_{15}^2 + \dot{q}_{16}^2 + \dot{q}_{17}^2 + \dot{q}_{18}^2 + \dot{q}_{19}^2 + \dot{q}_{20}^2 + \dot{q}_{21}^2) + \frac{5}{2} M_f \dot{q}_{22}^2$$

(Note that the total mass of the SNF is given by $5M_f$).

Lagrange's Equations of Motion have the general form

$$\frac{d}{dt} \left(\frac{\partial K}{\partial \dot{q}_i}\right) - \frac{\partial K}{\partial q_i} = Q_i \qquad i = 1,2...23$$

where K = the total kinetic energy of the system.

Since the component mass and inertia do not change with position during the seismic event, we have

$$\frac{\partial K}{\partial q_i} = 0 \qquad i = 1,2,...23$$

Using the above expressions for kinetic energy, we can carry out the differentiations

$$\frac{d}{dt}\left(\frac{\partial K}{\partial \dot{q}_i}\right) \qquad \text{where } K = K_1 + K_2 + K_3 + K_4$$

and set the result to Q_i, for i = 1,2...23 to obtain the 23 equations of motion for the system. In this application, the system is inertially decoupled (i.e., the final generalized mass matrix is diagonal); coupling is only through the various terms in the generalized force expressions. Nonlinear compression-only elements simulate contact and piecewise linear elements simulate friction between surfaces rendering the generalized forces nonlinear.

The final set of equations can be written in matrix form as

$$[M]\{\ddot{q}_i\} = \{Q_i(t)\}$$

where, the non-zero elements of the diagonal [M] are m_{ij} and

$$m_{11} = M_1 \; ; \; m_{22} = M_1 \; ; \; m_{33} = M_1$$

$$m_{44} = I_1 \; ; \; m_{55} = I_1 \; ; \; m_{66} = I_3$$

$$m_{77} = M_2 \; ; \; m_{88} = M_2 \; ; \; m_{99} = M_3$$

$$m_{10,10} = I_4 \; ; \; m_{11,11} = I_4$$

$$m_{12,12} = m_{13,13} = m_{14,14} = m_{15,15} = m_{16,16} = M_f$$

$$m_{17,17} = m_{18,18} = m_{19,19} = m_{20,20} = m_{21,21} = M_f$$
$$m_{22,22} = 5M_f \qquad m_{23,23} = M_4$$

The contributions to generalized force Q_i have spring-like behavior involving the difference between displacement components. Therefore, if all of the translational degrees of freedom are redefined to represent displacements relative to ground in the appropriate directions, then the generalized forces are unaltered. Therefore, the equations can be rewritten in terms of relative coordinates $p_i(t)$, where

$$p_i(t) = q_i(t) - U_1(t) \qquad i = 1,7,12,14,16,18,20$$

$$p_i\ (t) = q_i(t) - U_2(t) \qquad i = 2,8,13,15,17,19,21$$

$$p_i\ (t) = q_i(t) - U_3(t) \qquad i = 3,9,22,23$$

$$p_i(t) = q_i(t) \text{ all remaining (rotational) degrees of freedom}$$

The final system equations of motion are, in terms of $p_i(t)$, given as

$$[M]\ \{\ddot{p}_i\} = \{Q_i\ (p,t)\} - [M]\ \{U\}\ \ddot{U}_1\ (t) - [M]\ \{V\}\ \ddot{U}_2(t) - [M]\ \{W\}\ (\ddot{U}_3(t) + g)$$

with U(t) being the input ground acceleration time-histories, and where the column matrices {U}, {V}, {W}, consist of zero except as noted below.

$$\{U\}^T = [1,0,0,0,0,0,1,0,0,0,0,1,0,1,0,1,0,1,0,1,0,0,0]$$
$$\{V\}^T = [0,1,0,0,0,0,0,1,0,0,0,0,1,0,1,0,1,0,1,0,1,0,0]$$
$$\{W\}^T = [0,0,1,0,0,0,0,0,1,0,0,0,0,0,0,0,0,0,0,0,1,1]$$

Finally, the generalized forces can be developed in terms of the spring constants and the deformation of the springs associated with the simulation of contact or friction. In the Lagrangian formulation, the generalized forces for spring-like components can be written in the form

$$Q_i = -\sum_{J=1}^{NF} F_j\ (\Delta_j)\ \frac{\partial\ \Delta_j}{\partial\ q_i} \qquad i = 1,2,...23$$

where $F_j\ (\Delta_j)$ is a spring force associated with a kinematic extension Δ_j that arises due to contact or friction. The representation above allows for any $F_j\ (\Delta_j)$ to be zero during some time period due, for example, to loss of contact. For a given spring force representation identified by an extension Δ, the components

$$\frac{\partial \Delta_j}{\partial q_i}$$

can be identified by inspection of the particular Δ. The coefficients

$$\frac{\partial \Delta_j}{\partial q_i}$$

are labeled as the "coupling coefficients" associating a degree of freedom q_i to a particular spring force.

For example, for the cask with contact patch diameter d, then the "extension" of a vertical contact element at ground at the perimeter of the patch is given as

$$\Delta = q_3 + \frac{d}{2} \sin\theta \; q_4 - \frac{d}{2} \cos\theta \; q_5$$

where θ is measured in the horizontal plane from the x axis and locates the particular contact element around the edge. Therefore, for this particular contact spring, the coupling coefficients are, by inspection of Δ

$$\frac{\partial \Delta}{\partial q_3} = 1 \; ; \; \frac{\partial \Delta}{\partial q_4} = \frac{d}{2} \sin\theta \; ; \; \frac{\partial \Delta}{\partial q_5} = - \frac{d}{2} \cos\theta$$

The process of internally forming the generalized force matrix is built into Holtec International's QA-validated simulation code DYNAMO [7]; the user needs only to identify the various coupling coefficients for each spring.

For the application at hand, all spring forces can be written in the generic form

$$F_j = -K_j \, \Delta_j$$

where K_j is zero or non-zero based on the current state (tension or compression, restrained or sliding, etc.). The algorithm for establishing the current state of a spring force is also built into DYNAMO.

CHARACTERIZATION OF COULOMB FRICTION

The term "spring" in the lexicon of Component Element Dynamics [6] is any element in the structure which exerts a resistive force. The friction force, for example, is denoted as a "friction spring" with the bi-linear characteristic defined by

$$\begin{aligned} F &= N_H \text{ when } N_H < \mu \, N_v \\ &= \mu \, N_v \text{ when } N_H > \mu \, N_v \end{aligned}$$

where μ = coefficient of friction, and N_v and N_H are the vertical (compressive) and horizontal forces acting on the interface. Scores of analyses carried out on free-standing fuel rack structures for numerous nuclear plants show that the higher the coefficient of friction, the greater is the tendency of the structure to bind and tip over. Therefore, for conservatism, the value of μ is set at 0.8, which will increase the propensity for cask tipping. In addition to friction, the contact stiffness between the overpack and the ISFSI pad, S_1, and between various internal components of the HI-STAR 100 System (S_2 - S_4), need to be defined. The values of these springs should be established conservatively to ensure that the computed seismic response of the cask is overestimated.

A NUMERICAL EXAMPLE

For purposes of the numerical illustration of the method, the recently certified HI-STAR 100 [2] System is utilized. In particular, the response of a free-standing HI-STAR 100 System containing a loaded MPC-32 canister is considered. The principal input data necessary to characterize the physical problem is extracted from [2] and summarized in Table 1. Detailed computations to determine over a hundred input quantities needed to input in the dynamic model may be found in Reference [2]. In particular, the computation of the inertia properties of the various regions of the structure and evaluation of the contact spring stiffnesses involve tedious numerical work. The seismic accelerations applied in the three orthogonal directions are the previously discussed Regulatory Guide 1.60 inputs with a specific ZPA.

The computer Code DYNAMO [7], utilized for over twenty years in the dynamic simulation of free-standing structures under seismic excitations, has been utilized to implement the mathematical model described in the foregoing. To begin with, it is desired to establish the ZPA level at which HI-STAR 100 would be at the verge of "tipping over" at some instant during the

simulated seismic event. This sub-tipping ZPA for HI-STAR 100 was determined to be 0.6g, for which Figures 12 and 13, respectively, show the locus of the HI-STAR 100 centroid during the seismic event and the time-history rotation of its longitudinal axis with respect to a vertical axis. The locus of the cask (top center) is shown in Figure 14. It is seen that the maximum lateral rigid body motion at the top of the cask is approximately 70 inches from the initial location. Figures 15 and 16, respectively, show the total vertical contact force and horizontal shear force as a function of time.

Table 1: KEY HI-STAR DATA FOR DYNAMIC ANALYSIS	
Total Cask Weight	250,000 lbs
Cask Contact Patch Diameter, d_o	83.25 inches
MPC Outer Diameter	68.375 inches
Total Weight of Fuel Assemblies (MPC-32)	53,760 lbs
Weight of Overpack	153,080 lbs
Overpack Cavity Length	191.125 inch

Figure 12 shows that the HI-STAR 100 centroid remains *within* the initial contact patch circle during the entire seismic event. Figure 13 shows that the maximum departure of the cask axis from the vertical is 20 degrees (0.348 radians), which is slightly less than the limiting (C.G.-over-the-corner) excursion of 22.5 degrees. Therefore, it is concluded that the 3-D Reg. Guide 1.60 seismic accelerations with ZPA = 0.6g will not tip the cask.

Figure 15 shows the variation of net vertical force at the cask-pad interface during the time duration of the event for the seismic event. The total force is obtained by summing the forces in the vertical "compression-only" spring elements representing the cask-to-storage pad interface at each instant in time and plotting the resulting force vs. time. Dividing the peak force by the weight of the system gives a measure of the peak vertical deceleration experienced by the cask. A similar summation over time of the friction forces at the interface in the two horizontal directions yields a measure of the net horizontal force experienced by the cask system over time (Figure 16).

Dividing the peak vertical and horizontal forces by the mass of the cask gives the vertical and horizontal accelerations sustained by the system during the seismic event.

We have

$$\text{Vertical acceleration } a_v = \frac{1{,}366{,}290}{250{,}000} = 5.46$$

To study the effect of reduced ZPA loadings, the case of ZPA = 0.45g was also analyzed.

Figures 17 and 18, respectively, show the locus of the top centerpoint and centroid of the cask. The maximum excursion of the top of the cask is now only 9 inches (compared to 70 inches at 0.6g event). As shown in Figure 19, the maximum rotation of the cask longitudinal axis is reduced to 4.93 degrees, which is a little over 20% of the tip-over incipience angle (22.5 degrees). These results illustrate that a mere one-third reduction in the ZPA level (from 0.6 to 0.45) causes over a fourfold reduction in the cask kinematic response.

Figure 20 shows a plot of the maximum angular departure of the cask axis from the vertical, ψ, as a function of the ZPA level. Figure 20 shows that the response of the cask does not increase monotonically with the "strength" of the earthquake, which is not an unexpected result for a nonlinear structure.

PROPOSED ACCEPTANCE CRITERIA

At present, there are no regulatory criteria to define acceptable seismic events other than the static "no tip" criterion. We herein present design criteria which may be considered by the regulatory authorities for possible adoption.

There are four distinct limitations which should be placed on the acceptable cask response. They are:

i. Restriction on the maximum sliding, δ, of the cask.
ii. Restriction on the maximum rotation (overturning) angle of cask centerline, ψ.
iii. Restriction on the maximum fuel assembly to storage cell impact load, F.
iv. Restriction on the maximum deflection of the storage cell wall due to rattling at the cell wall/SNF interface.

Proposed limits on the above response variables are given below.

Sliding Limits: As we show using the numerical example of HI-STAR 100, limiting the maximum displacement δ to 25% of the cask contact circle ensures that the DBE will be well within the "stable" zone.

Axial Tilt, ψ: Restricting the maximum axial tilt of the cask to 25% of the incipient tipping angle, as we show using the HI-STAR 100 example, ensures that the DBE event is well within the "stable" zone.

SNF/Fuel Cell Impact Load, F: The impact load between the SNF and the storage cell due to rattling of the fuel during the seismic event should not exceed the maximum value specified by the fuel supplier.

Basket Cell Wall Stress: In order to ensure that the storage cell walls do not sustain deformations leading to violation of the provisions of the applicable section of 10CFR72, the maximum stress level in the basket cell walls should be limited to Level D limits of the ASME Code for Subsection "NG" components.

CLOSURE

A method to predict the seismic response of free-standing spent fuel storage casks under a three-dimensional seismic excitation has been presented. A storage cask containing a "free-to-rattle" canister basket and nuclear fuel assemblies is an epitome of a nonlinear structure. Furthermore, the range of variations in variables with potentially significant effect on the cask response can be quite large. For example, the cask-to-ISFSI pad interfacial coefficient of friction can vary within a large range (as low as 0.1 in a wet interface to 0.8 in dry rough conditions). The analysis methodology presented herein enables the analyst to make parametric analyses to establish the most pessimistic (maximum displacement and/or rotation) cask response. Exploratory analyses on a HI-STAR 100 System show that the cask response is a highly nonlinear function of the ZPA of the seismic event. After a certain threshold value, the response (viz. maximum tilting of the cask axis) increases rapidly with increase in the ZPA level. For this reason, it is recommended that the acceptable response parameters, e.g., maximum rotation of the cask axis, be set at one-fourth of the "ultimate" value (at which the cask will tip beyond the C.G.-over-corner orientation). In addition to kinematic limits, specific requirements on stress limits in critical cask contents are also proposed.

While the methodology is developed for the general case of free-standing casks, special cases, such as the case of anchored casks, can be analyzed using this method without any difficulty.

The standard Regulatory Guide 1.60 spectrum was used for purposes of illustration. For a specific storage site, however, the applicable DBE is available from the local seismic analyses. The analysis of the seismic behavior of a cask for the site can be performed using the dynamic model described in this paper and the acceleration time-histories applicable to the ISFSI. The acceptance criteria proposed in this paper may be used to determine whether the kinematic response of the cask is admissibly small to permit a free-standing installation. The interface forces between the cask and the ISFSI pad obtained from the time-history analysis can be used in the structural design of the reinforced concrete ISFSI pad.

NOMENCLATURE

I_1	mass moment of inertia of overpack about x or y axis through the centroid
I_3	mass moment of inertia of overpack about z axis through the centroid
I_4	mass moment of inertia of MPC (canister plus fuel basket) about x or y axis through the centroid
K_i	kinetic energy of i^{th} component (i = 1 overpack, i = 2 MPC, i = 3 fuel basket vertical motion, i = 4 fuel assembly)
M_1	mass of overpack
M_2	mass of MPC (canister plus fuel basket)
M_3	mass of MPC enclosure vessel
M_4	mass of fuel basket
Q_i	generalized force for i^{th} degree of freedom
q_1 - q_6	overpack translational and rotational degrees of freedom
q_7 - q_{11}	MPC translational and rotational degrees of freedom
q_{12} - q_{21}	fuel translational (horizontal) degrees of freedom
q_{22}	vertical degree of freedom of stored SNF
q_{23}	fuel basket vertical degree of freedom
S_1	overpack-to-ISFSI pad contact stiffness
S_2	fuel basket-to-fuel assembly contact stiffness
S_3	MPC-to-overpack bottom plate contact stiffness
S_4	fuel basket-to-MPC contact stiffness
U_j (j=1,2,3)	ground displacement (functions of time)
μ	overpack/bearing pad interface friction coefficient

REFERENCES

[1] NRC Information Notice 95-28, "Emplacement of Support Pads for Spent Fuel Dry Storage Installations at Reactor Sites, USNRC," Washington, D.C. (1995).

[2] Topical Safety Analysis Report for HI-STAR 100, Holtec Report No. HI-941184, Rev. 4 (September 1996).

[3] USNRC Regulatory Guide 1.60, Design Response Spectra for Seismic Design of Nuclear Power Plants.

[4] K.P. Singh and A.I. Soler, "Mechanical Design of Heat Exchangers and Pressure Vessel Components", Chapter 21, Arcturus Publishers, Cherry Hill, NJ, 1984.

[5] Dynamics of Structures, by R.W. Clough and J. Penzien, p. 273, McGraw Hill (1975).

[6] S. Levy and J. Wilkenson, The Component Element Method in Dynamics, McGraw-Hill, 1976.

[7] Holtec Proprietary Computer Code DYNAMO, QA Validation Manual, HI-91700, 1991.

[8] United States Nuclear Regulatory Commission, NUREG-0800, SRP 3.7.5, Washington, D.C. (1981).

[9] "Nuclear Reactors and Earthquakes", Oak Ridge National Laboratory, ORNL 3468 (1963).

[10] "Seismic Response of a Free Standing Fuel Rack Construction to 3-D Floor Motion", Alan I. Soler and Krishna P. Singh, Nuclear Engineering and Design (1984).

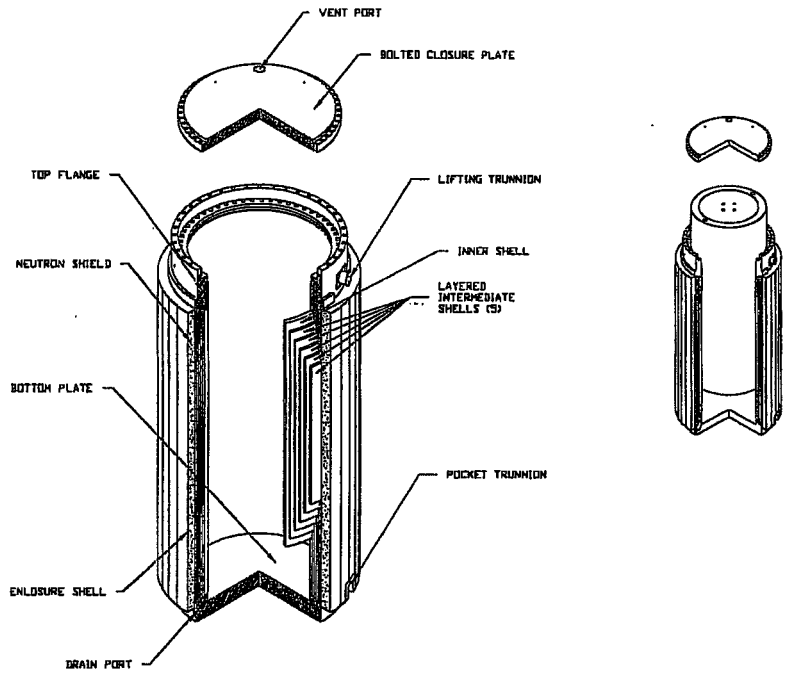

FIGURE 1 PICTORIAL VIEW OF HI-STAR 100 OVERPACK WITH MPC PARTIALLY INSERTED

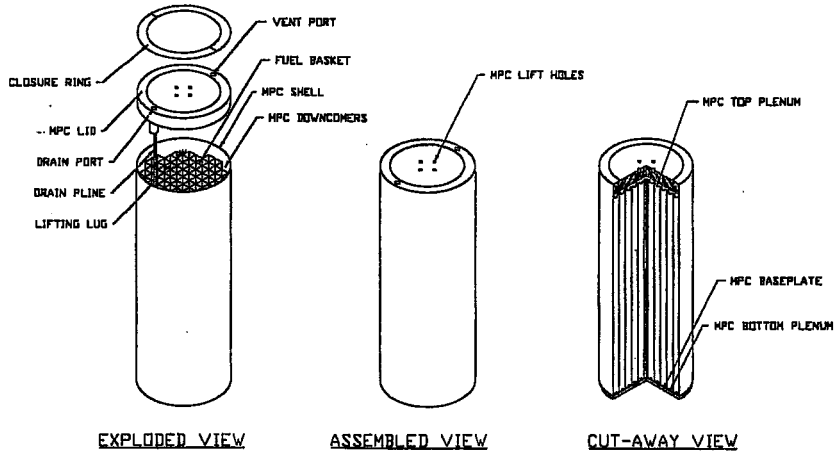

FIGURE 2 THE HI-STAR 100 AND HI-STORM 100 MPC SYSTEM

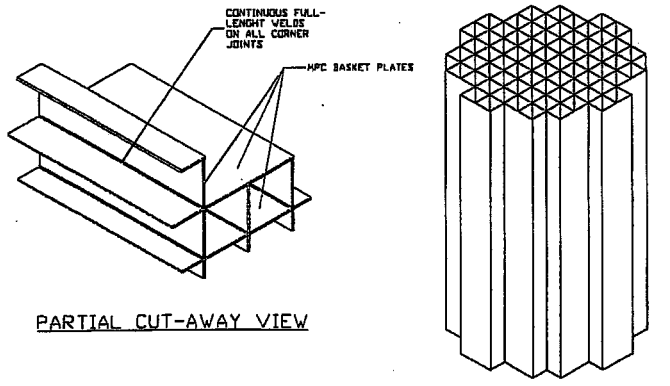

FIGURE 3 PICTORIAL VIEW OF A FUEL BASKET

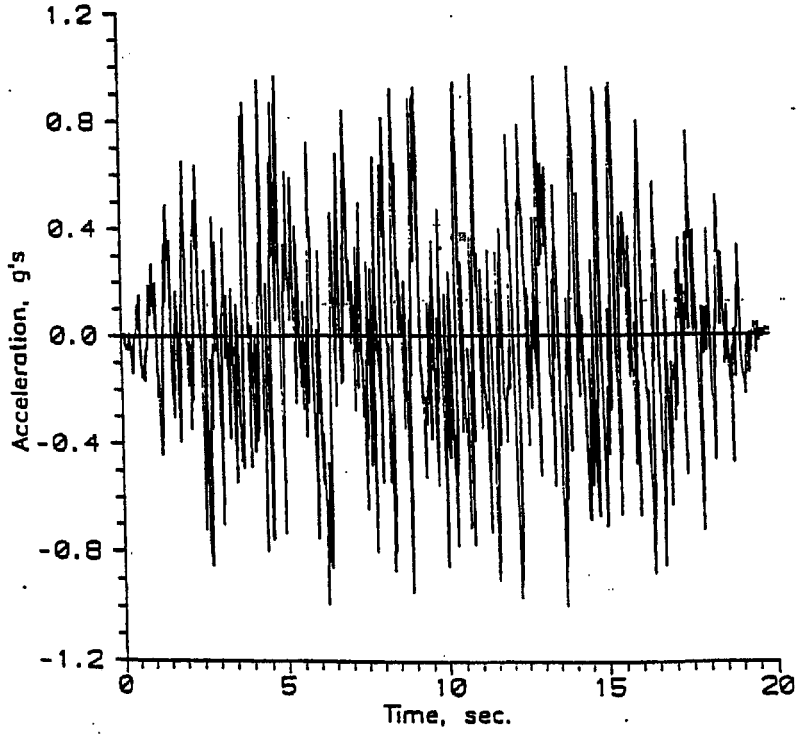

FIGURE 4 **STANDARD SYNTHETIC ACCELERATION TIME-HISTORY ACCELT.H1, SYNTHESIZED FROM THE REGULATORY GUIDE 1.60 HORIZONTAL RESPONSE SPECTRUM**

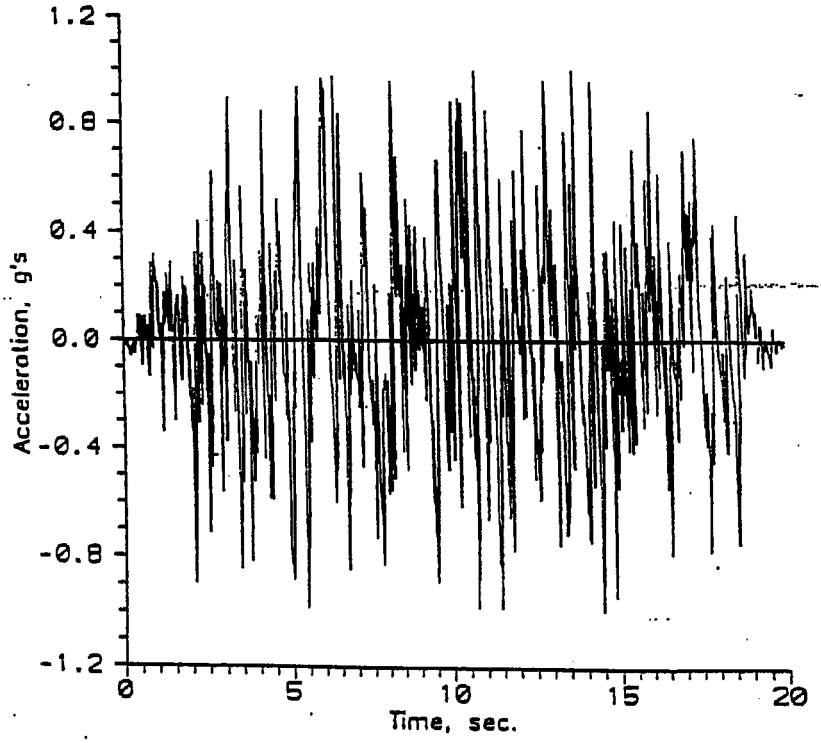

FIGURE 5 STANDARD SYNTHETIC ACCELERATION TIME-HISTORY ACCELT.H2, SYNTHESIZED FROM THE REGULATORY GUIDE 1.60 HORIZONTAL RESPONSE SPECTRUM

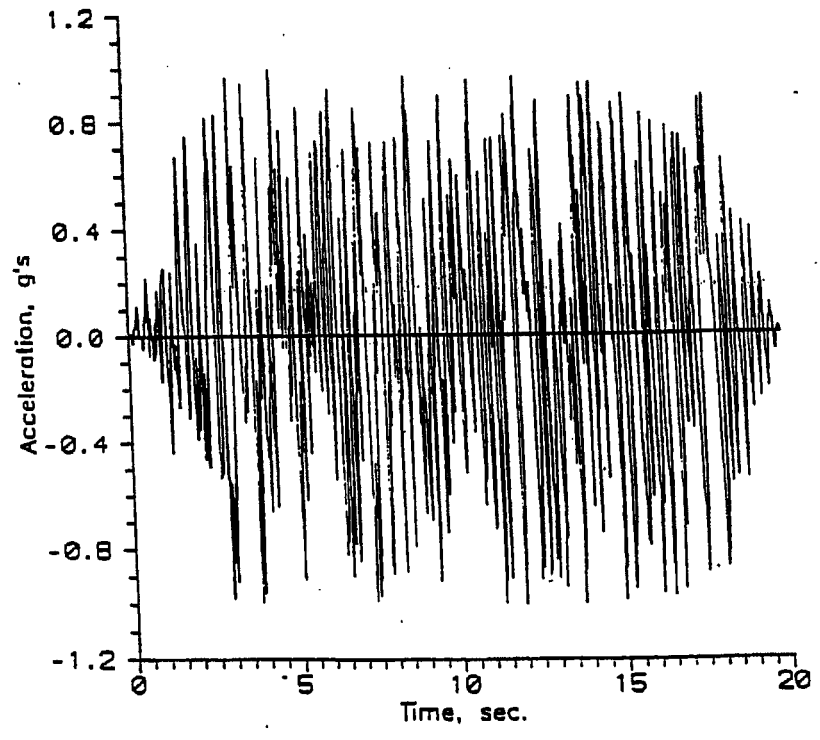

FIGURE 6 STANDARD SYNTHETIC ACCELERATION TIME-HISTORY ACCELT.VT, SYNTHESIZED FROM THE REGULATORY GUIDE 1.60 HORIZONTAL RESPONSE SPECTRUM

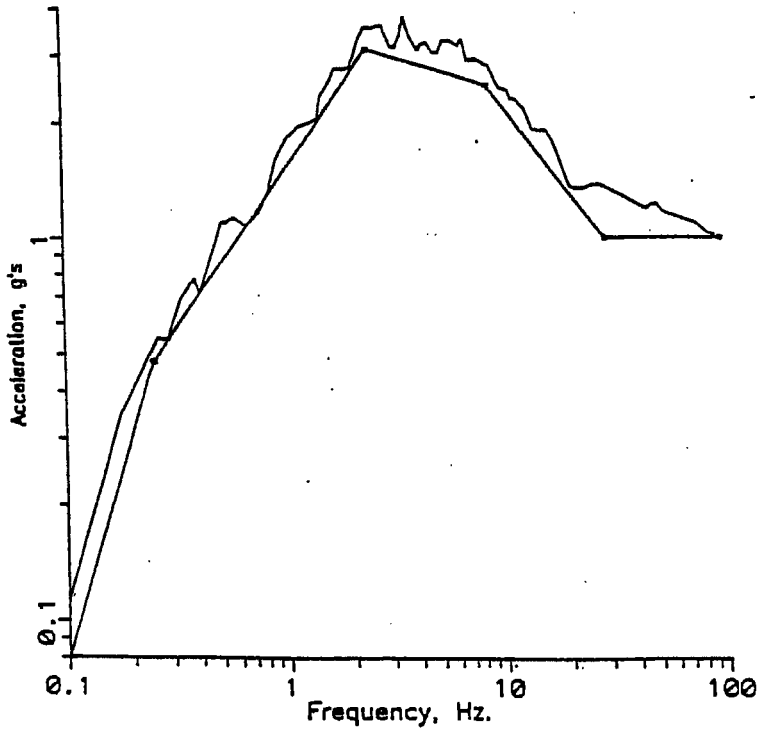

FIGURE 7 RESPONSE SPECTRUM OF SYNTHETIC ACCELERATION TIME-HISTORY ACCELT.H1 AND THE ORIGINAL SSE RESPONSE SPECTRUM (5% DAMPING)

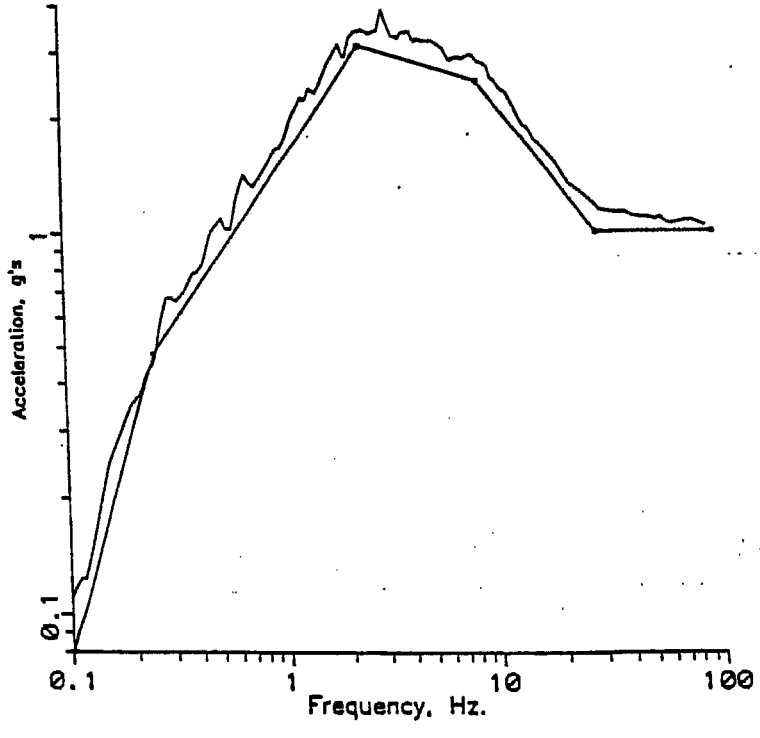

FIGURE 8 RESPONSE SPECTRUM OF SYNTHETIC ACCELERATION TIME-HISTORY ACCELT.H2 AND THE ORIGINAL SSE RESPONSE SPECTRUM (5% DAMPING)

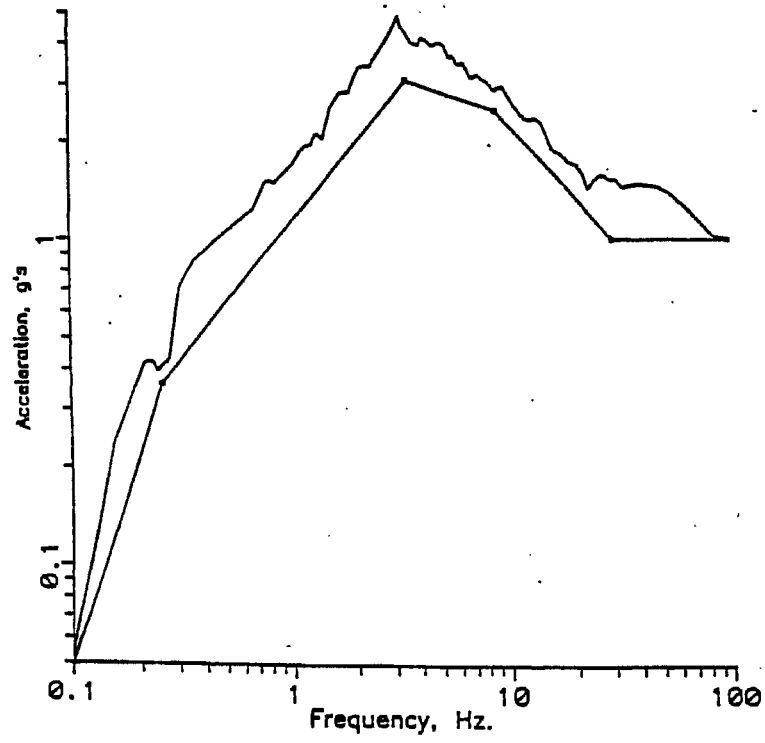

FIGURE 9 **RESPONSE SPECTRUM OF SYNTHETIC ACCELERATION TIME-HISTORY ACCELT.VT AND THE ORIGINAL SSE RESPONSE SPECTRUM (5% DAMPING)**

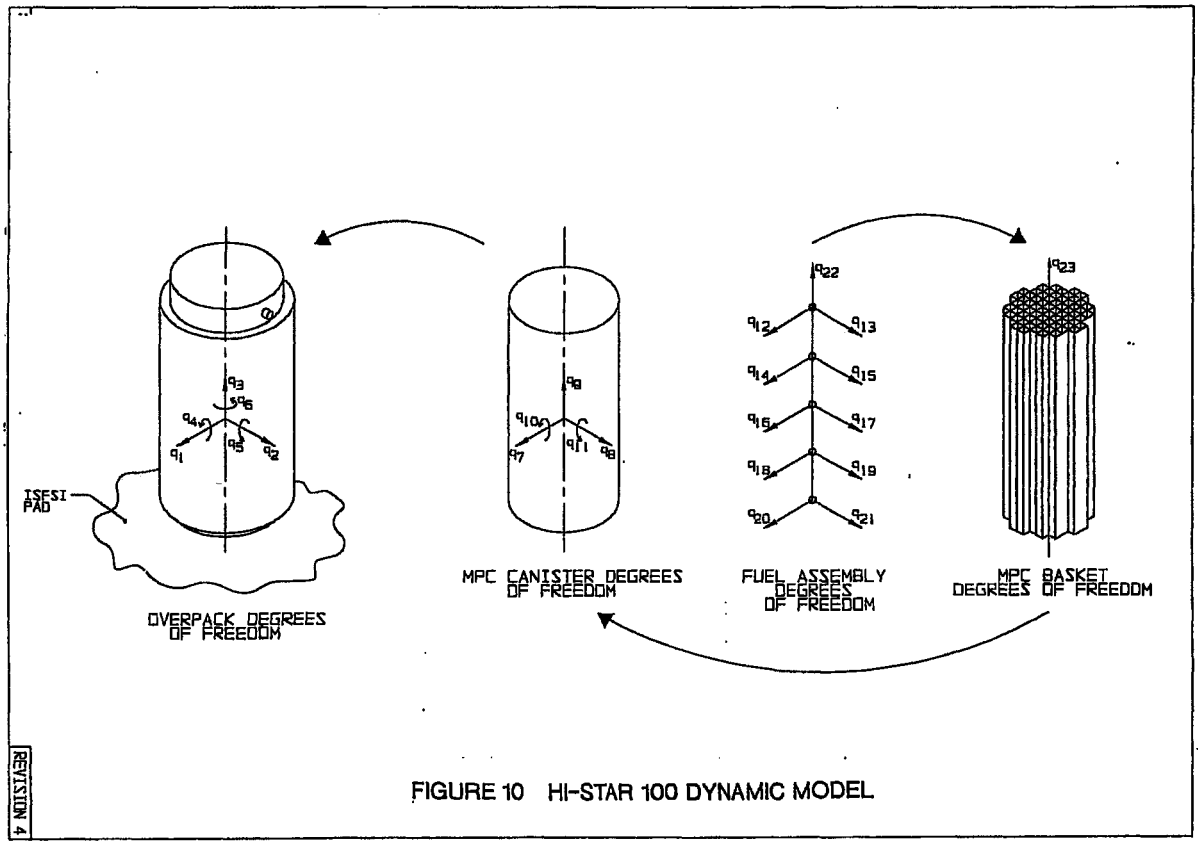

FIGURE 10 HI-STAR 100 DYNAMIC MODEL

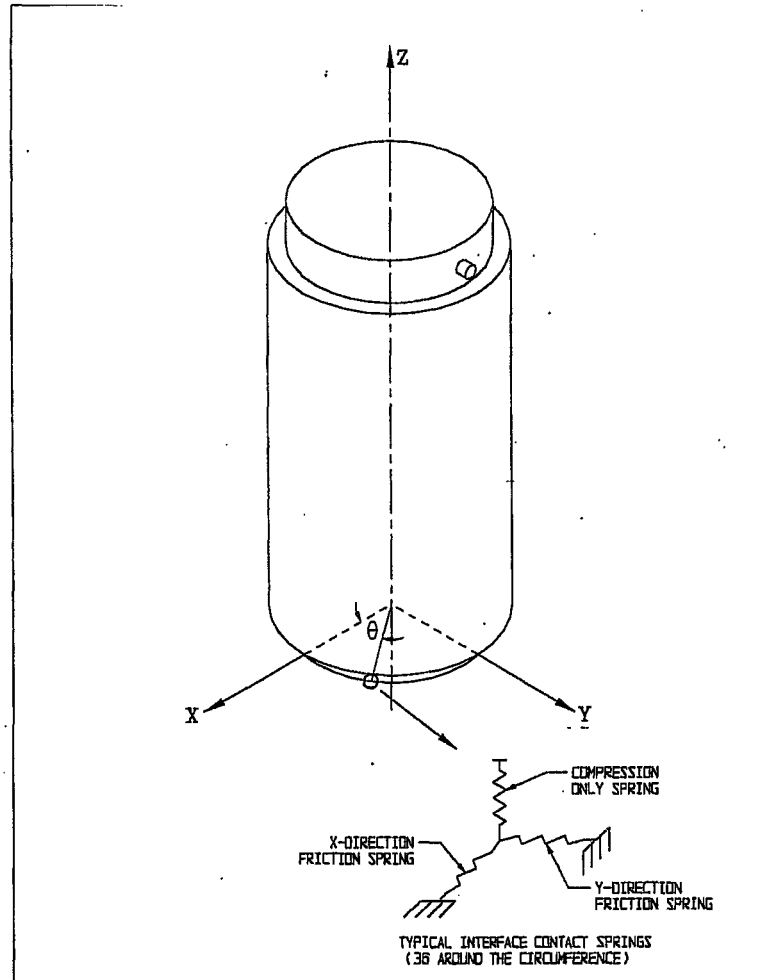

FIGURE 11 CASK-ISFSI PAD INTERFACE CONTACT ELEMENTS

REVISION 4

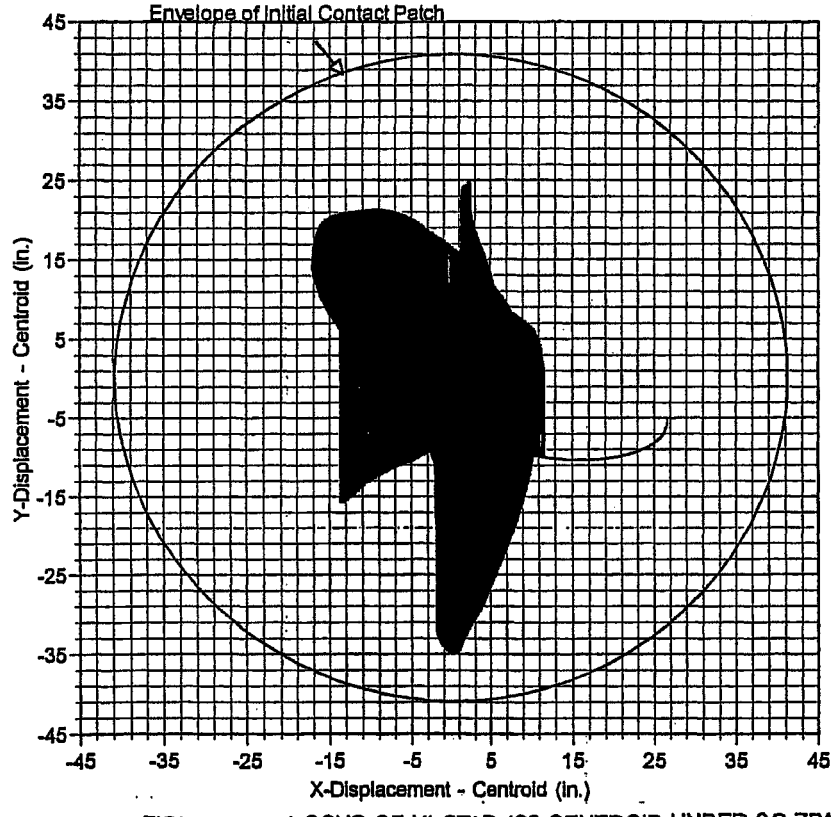

FIGURE 12 LOCUS OF HI-STAR 100 CENTROID UNDER 0.6 ZPA REG. GUIDE 1.60 3-D SEISMIC EVENT

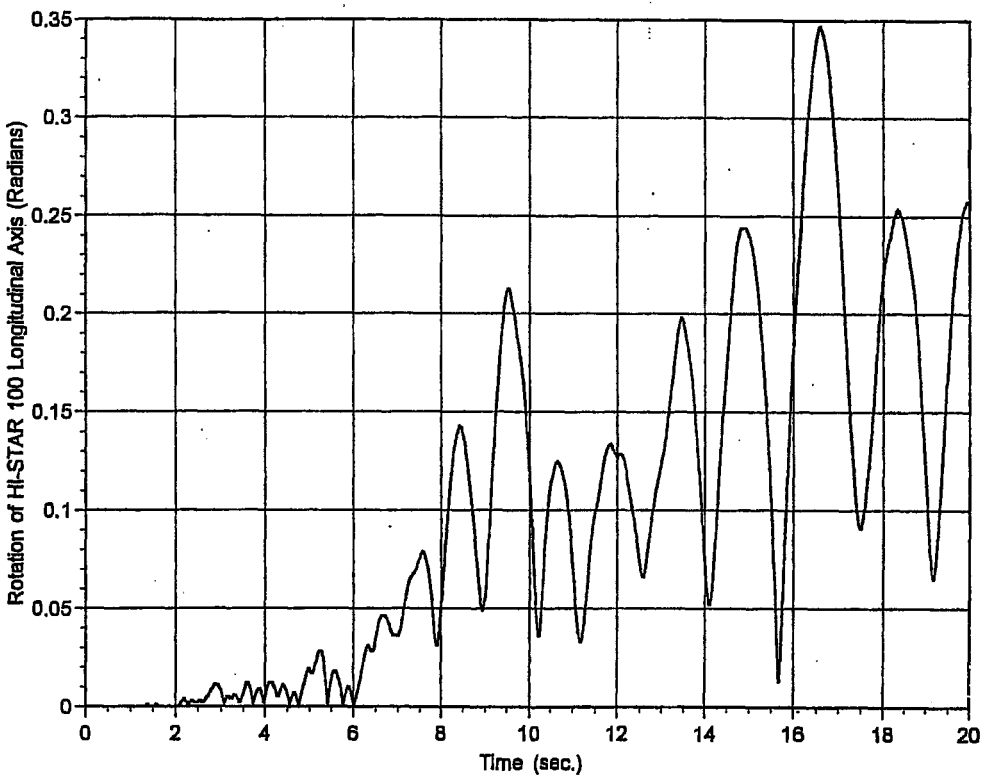

FIGURE 13 RIGID BODY ROTATION OF HI-STAR 100 AXIS WITH TIME UNDER 0.6g ZPA REG. GUIDE 1.60 3-D SEISMIC MOTION

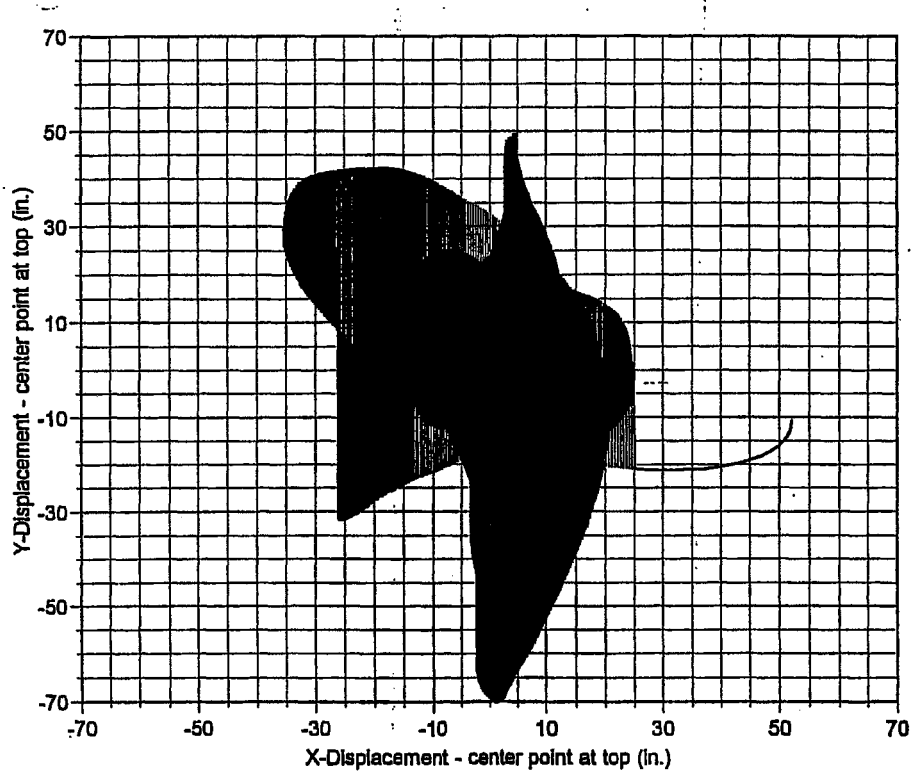

FIGURE 14 LOCUS OF HI-STAR 100 TOP CENTER POINT

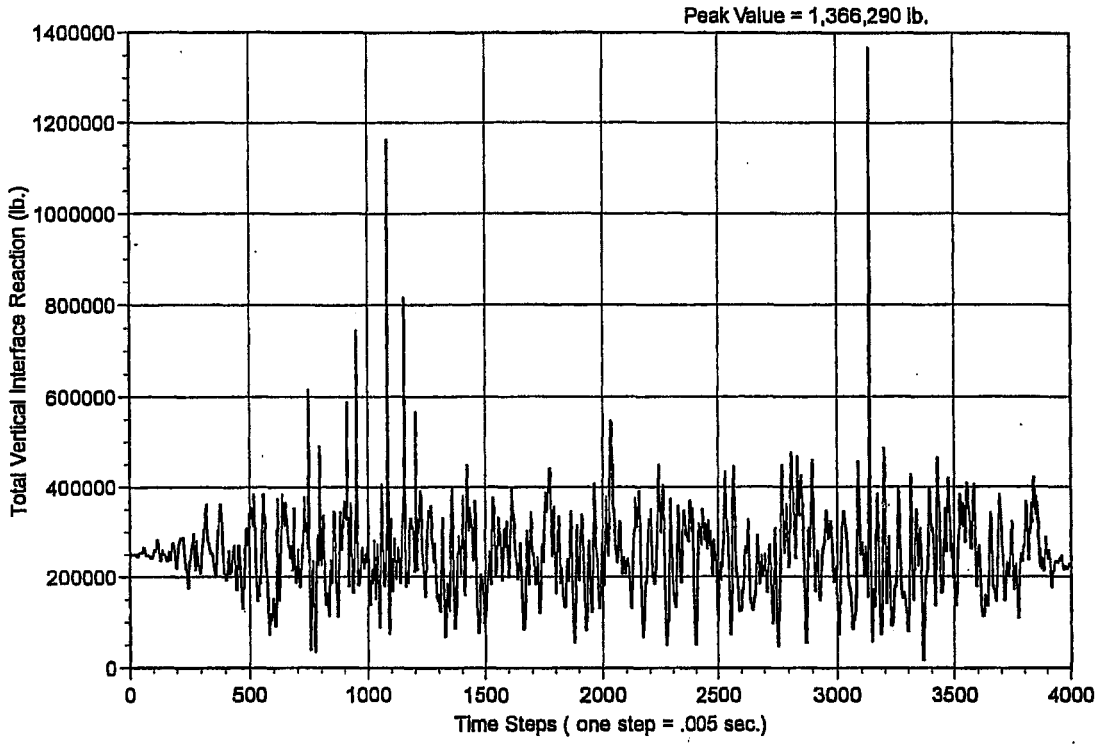

FIGURE 15 TOTAL VERTICAL CONTACT LOAD VS. TIME (SUM OF 36 LOCATIONS)

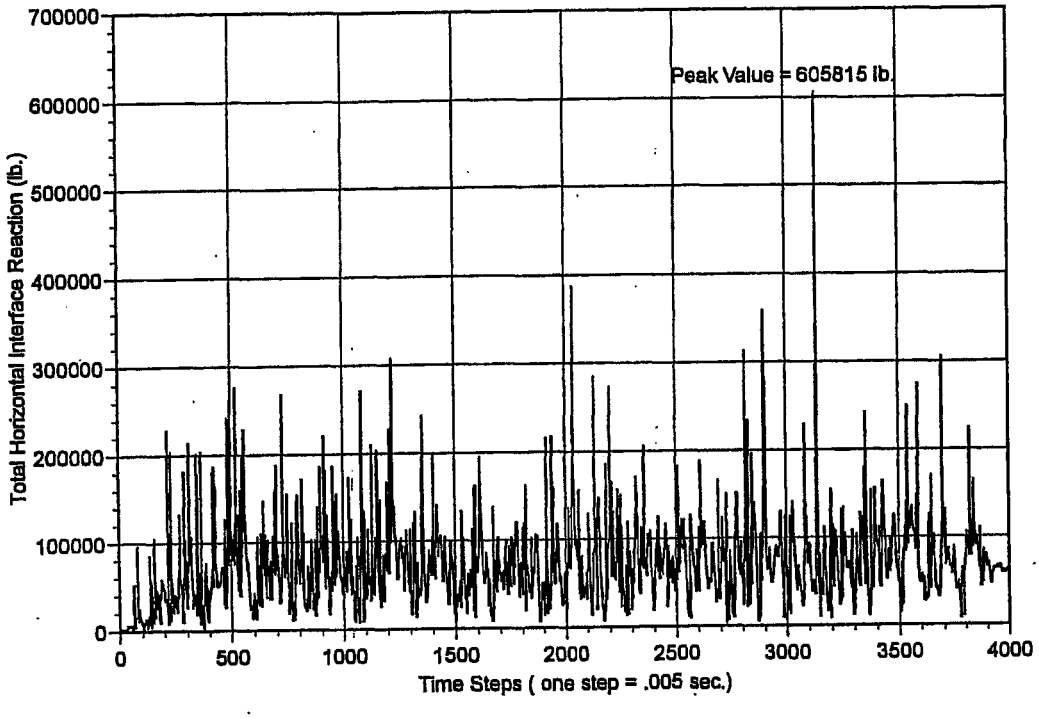

FIGURE 16 TOTAL VECTORIAL HORIZONTAL CONTACT LOAD VS. TIME

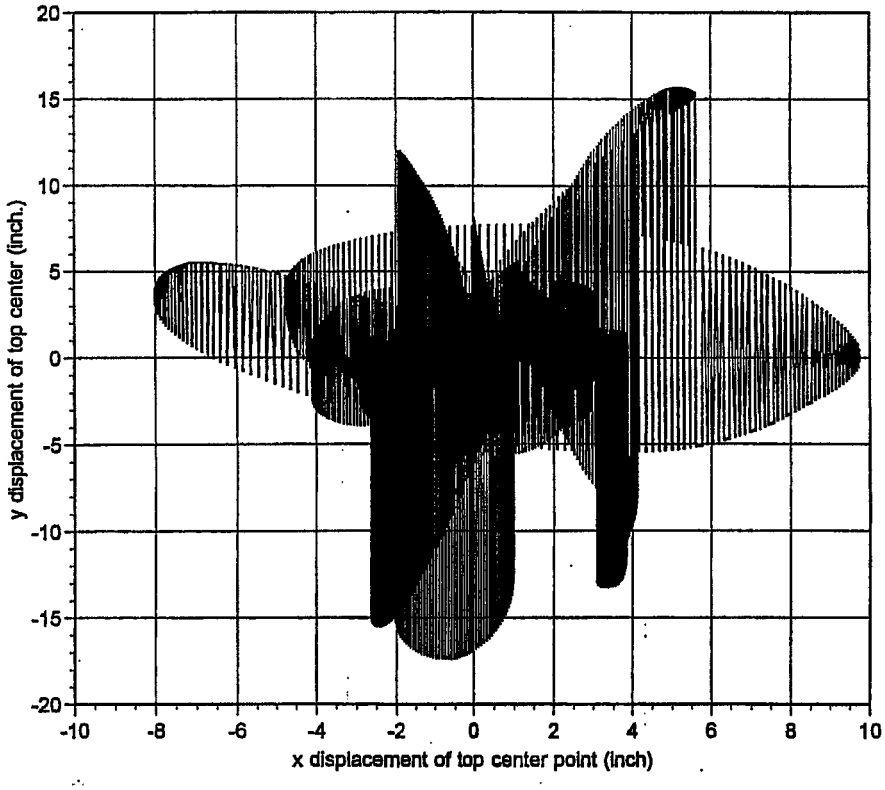

FIGURE 17 LOCUS OF TOP CENTER POINT – .45G REG. GUIDE 1.60 EVENT

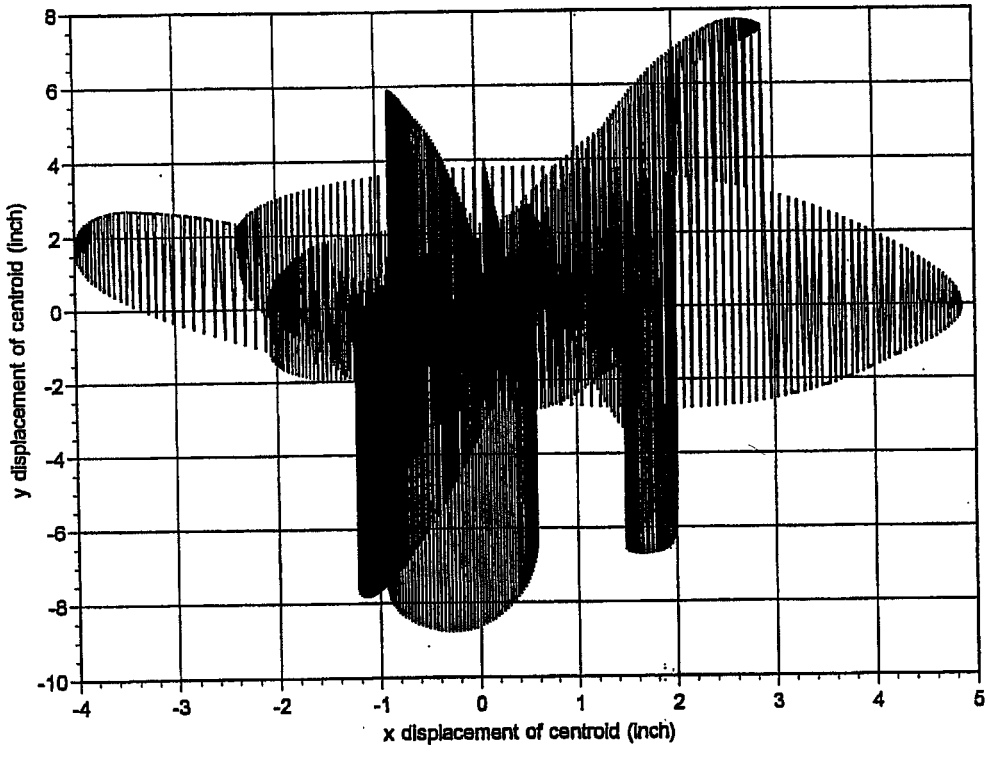

FIGURE 18 LOCUS OF HI-STAR 100 CENTROID – .45G REG. GUIDE 1.60 EVENT

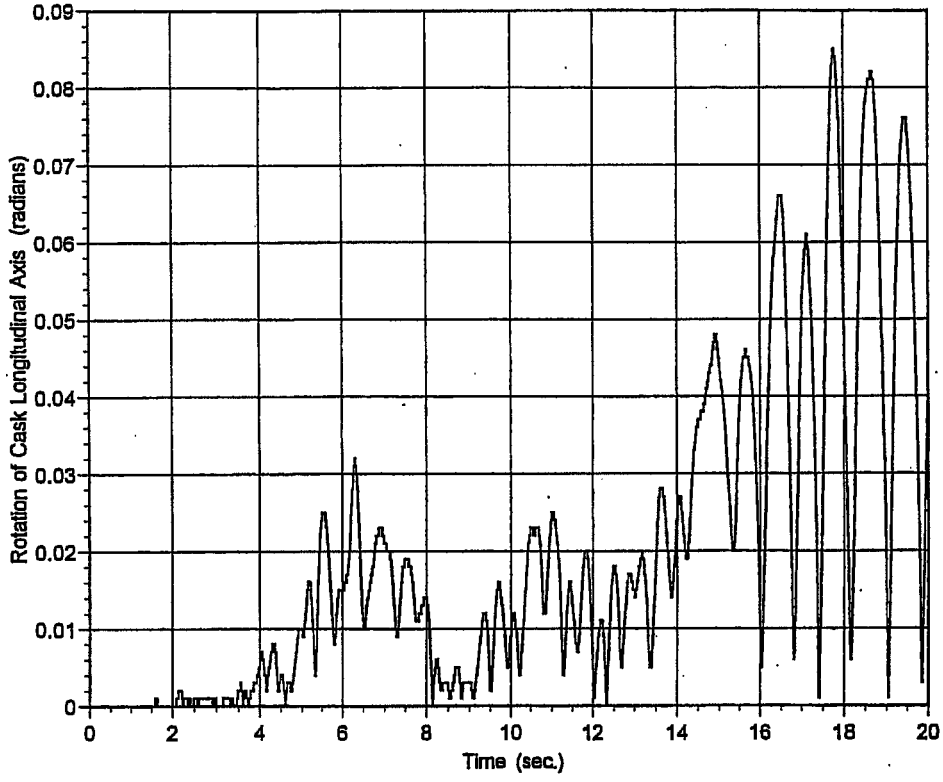

FIGURE 19 ROTATION OF HI-STAR 100 LONGITUDINAL AXIS VS. TIME .45G REG. GUIDE 1.60 EVENT

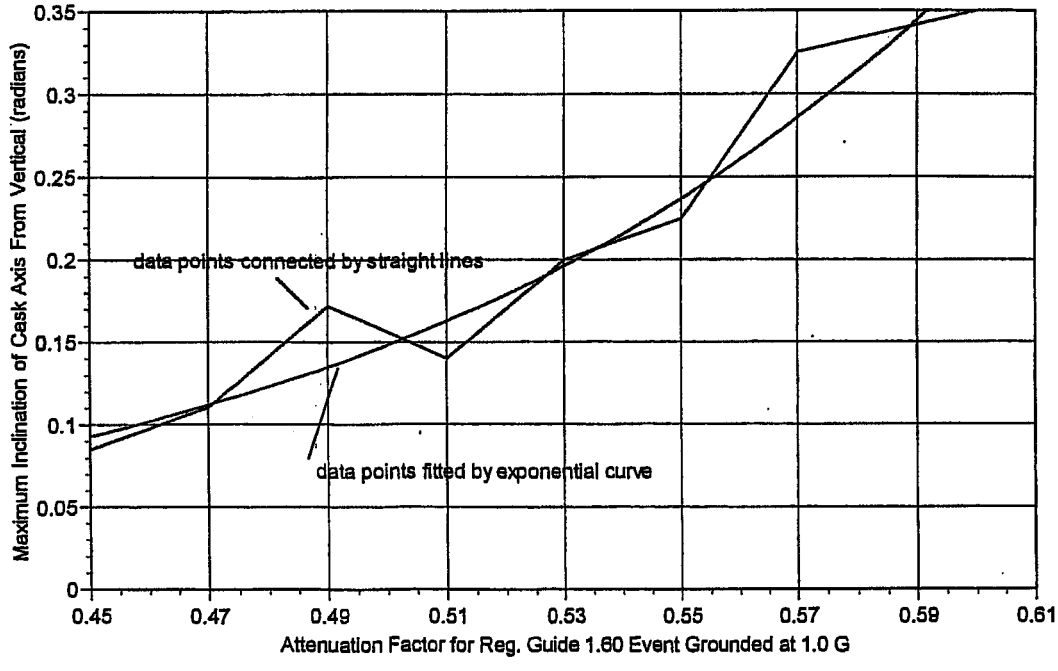

FIGURE 20 MAXIMUM ANGLE OF INCLINATION OF CASK LONGITUDINAL AXIS VS. REG. GUIDE 1.60 ZPA